Int. J. Multiphase Flow Vol. 19, No. 5, pp. 905–912, 1993
Printed in Great Britain.

0301-9322/93 $6.00 + 0.00

AN APPROXIMATE SOLUTION OF THE HYDRODYNAMIC PROBLEM ASSOCIATED WITH RECEDING LIQUID–GAS CONTACT LINES

A. K. CHESTERS and A. J. J. VAN DER ZANDEN
Laboratory of Fluid Dynamics and Heat Transfer, Eindhoven University of Technology, P.O. Box 513, Eindhoven, The Netherlands

(Received 15 February 1991; in revised form 22 June 1993)

Abstract—An ordinary differential equation, derived previously by the authors to describe liquid–gas menisci in the context of advancing contact lines, is applied to the receding case. The existence of a critical capillary number is demonstrated above which no solution of the differential equations exists. This critical capillary number exhibits a strong dependence on the system scale and true contact angle at the wall. Comparison of critical capillary numbers, predicted by the model and obtained from experiments, suggests that at the critical capillary number the true contact angle at the wall is smaller than the (receding) static contact angle.

Key Words: wetting, dewetting, dynamic contact line

1. INTRODUCTION

While advancing liquid–gas contact lines have been the subject of attention for some time, most research into receding lines is relatively recent. The most striking feature of receding contact lines, in contrast with advancing contact lines, is the existence of a maximum speed of dewetting as demonstrated experimentally by Blake & Ruschak (1979). For small capillary numbers, Ca (Ca $= \mu U/\sigma$, where μ—dynamic viscosity of the liquid, U—line speed and σ—surface tension), a hydrodynamic description was given by Voinov (1976, 1978), de Gennes (1986), Cox (1986) and Teletzke *et al.* (1988), the latter incorporating not only hydrodynamics but also disjoining pressure. Spontaneous dewetting of a parallel film on plane surfaces has been described by Brochard *et al.* (1988), Brochard-Wyart & Daillant (1990), Redon *et al.* (1991) and of film on fibres by Brochard-Wyart *et al.* (1987). A few experimental studies examined the receding contact line by withdrawing a polyester tape (Petrov & Sedev 1985) or a glass rod (Sedev & Petrov 1988/89, 1991) from a liquid. Receding contact lines with surfactants were studied by Petrov & Radoev (1981), de Gennes (1986) and Hopf & Geidel (1987). Receding contact lines in the geometry of a capillary have not been the subject of a large number of studies. Rillaerts & Joos (1980) examined experimentally almost exclusively advancing contact angles in a tube. They reported that "the receding contact angle became rapidly zero". One study of Quéré (1991) examined experimentally the relation between the static contact angle and the Ca at which a film starts being left behind, the critical capillary number (Ca_{crit}).

In the present article a simplified approach to the hydrodynamics of moving contact lines, developed earlier in the context of advancing lines without restriction on the magnitude of Ca [Boender *et al.* (1991)—henceforth referred to as paper I], is applied to the problem of a steadily receding liquid–gas contact line. The approach supposes the system length scale to be sufficiently small and the liquid sufficiently viscous for gravitational and inertial stresses to be negligible in the liquid and all stresses, aside from a uniform pressure, to be negligible in the gas.

Like other analyses of the line-speed dependence of the apparent (or "dynamic") contact angle, the region adjoining the line is split into a region in which the classical concepts of surface tension and the continuum approximation apply and a region very close to the line in which one or more of these concepts breaks down [see Dussan (1979) and de Gennes (1985) for relatively recent reviews]. In the former region, the approach developed in paper I reduces the free-surface hydrodynamic problem relating to a second-order ordinary differential equation for the variation of meniscus inclination with distance from the wall by making use of the fact that this variation

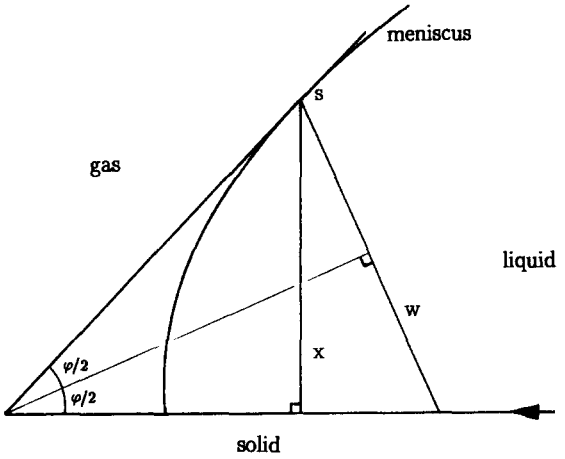

Figure 1. Definition of the variables for a receding meniscus.

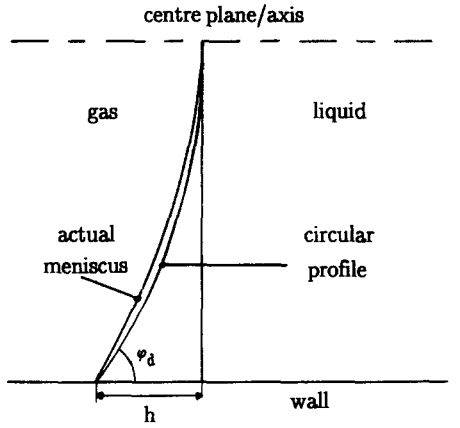

Figure 2. Definition of the dynamic contact angle, φ_d.

is typically slow in an appropriate dimensionless sense, so that analytical solutions for the flow and pressure variation in a plane wedge are applicable locally. The existence of the non-classical region was incorporated in paper I by including the only feature known with certainty—that the continuum description, and with it concepts such as the meniscus inclination, loses its validity at a distance from the wall minimally of the order of a molecular dimension. The meniscus inclination at this distance from the wall, the true contact angle, was furthermore for simplicity's sake supposed to be adequately approximated by the equilibrium (static) value.† The latter assumption was not, however, severely tested by the ensuing comparison of predicted and measured dynamic angles, since for the large line speeds at which an appreciable deviation from the static angle might be expected the dynamic angle proves relatively insensitive to the value of the true angle.

The meniscus equation derived in paper I contains no assumption as to the sign of the line speed and is consequently applicable to receding liquid–gas contact lines as well. The meniscus equation is presented in section 2 and its numerical solution in the receding case explored in section 3. In sections 4 and 6 the corresponding implications for the dependence of the dynamic contact angle on line speed, true contact angle and system scale are investigated. In section 5 the validity of the model is examined. In section 7 predictions of Ca_{crit} are compared with the experiments of Quéré (1991).

2. THE DIFFERENTIAL EQUATIONS DESCRIBING RECEDING MENISCI

With respect to a reference frame moving with the contact line, a receding meniscus may be described by means of the coordinates x and φ (figure 1, φ in radians). Neglecting gravitational and inertial forces, the differential equation describing an *advancing* meniscus between two parallel planes, when a viscous liquid replaces a gas over a smooth homogeneous surface, is shown in paper I to be

$$\frac{1}{A(\varphi)\sin\varphi}\frac{d}{dx}\left(\sin\varphi\frac{d\varphi}{dx}\right)=\frac{-Ca}{x^2}, \qquad [1]$$

where

$$A(\varphi)=\frac{-2\sin\varphi}{\sin\varphi\cos\varphi-\varphi} \qquad [2]$$

and

$$Ca=\frac{\mu U}{\sigma} \qquad [3]$$

is the dimensionless line speed, or capillary number (μ, U and σ are the viscosity of the advancing fluid, the speed of the contact line and the surface tension, respectively). As noted above, [1] is based

†The solid is supposed to be perfectly smooth and chemically homogeneous, resulting in equal advancing and receding static angles. In reality a certain hysteresis is always present (see section 7).

on a local-wedge approximation for the flow and pressure gradient which should be acceptable provided that angle φ varies slowly in a dimensionless sense:

$$\frac{\dfrac{\mathrm{d}\varphi}{\varphi}}{\dfrac{\mathrm{d}s}{w}} \ll 1 \qquad [4]$$

(s and w are the arc length along the meniscus and the local wedge width, respectively: figure 1).

The derivation of [1] places no restriction on the sign of the line speed and [1] thus also applies to a receding meniscus (Ca < 0), provided [4] is satisfied. (With $U < 0$, μ becomes the viscosity of the receding fluid.)

Likewise the differential equation describing an advancing meniscus in a tube,

$$\frac{\mathrm{d}}{\mathrm{d}x}\left(\sin\varphi\frac{\mathrm{d}\varphi}{\mathrm{d}x}+\frac{\cos\varphi}{a-x}\right)=\frac{-\mathrm{Ca}\,A(\varphi)\sin\varphi}{x^2} \qquad [5]$$

(in which a is the tube radius), derived in paper I, should be applied to the receding case also.

The boundary conditions to be satisfied by [1] or [5] at the wall are again taken to be

$$\varphi = \varphi_0, \quad \text{at } x = \lambda, \qquad [6]$$

where λ is a distance minimally of the order of a molecular dimension and φ_0 the true contact angle. Alternatively, λ and φ_0 may be viewed as phenomenological parameters whose magnitude must be determined from experiment and whose interpretation must await more detailed consideration of the region adjoining the line. As discussed in the advancing case, there is no *a priori* justification for the assumption that φ_0 remains equal to the static contact angle, φ_s. Furthermore, in contrast to the advancing case, any variation of φ_0 with line speed proves of major influence on the apparent or "dynamic" contact angle, φ_d, in the receding case.

In paper I the dynamic contact angle is defined as the angle obtained if the central, circular profile of the meniscus is extrapolated to the wall. In the receding case a closely circular central profile is often absent and a more practical definition is the angle which a circular/spherical meniscus having the same apex height h as the actual meniscus makes with the wall (figure 2):

$$\varphi_\mathrm{d} = \cos^{-1}\left(\frac{-2ha}{a^2+h^2}\right). \qquad [7]$$

In cases in which a large spherical portion exists the two definitions of φ_d become equivalent.

3. SOLUTION OF THE MENISCUS EQUATION

The differential equations [1] and [5] are solved as indicated in paper I, making use of a logarithmic scale of distance,

$$\xi = \ln\left(\frac{x}{\lambda}\right), \qquad [8]$$

by numerically integrating from the centreline/centre axis ξ_c to the distance λ from the wall ($\xi = 0$) using a second-order finite-difference scheme. The subscript c is used to identify a property on the centre plane/centre axis and the subscript 0 a property at $\xi = 0$. The integration procedure requires the values of φ_c and η_c, where

$$\eta = \frac{\mathrm{d}\varphi}{\mathrm{d}\xi}. \qquad [9]$$

Symmetry requires that φ_c be 90°. The value of η_c determines the value of φ_0 obtained.

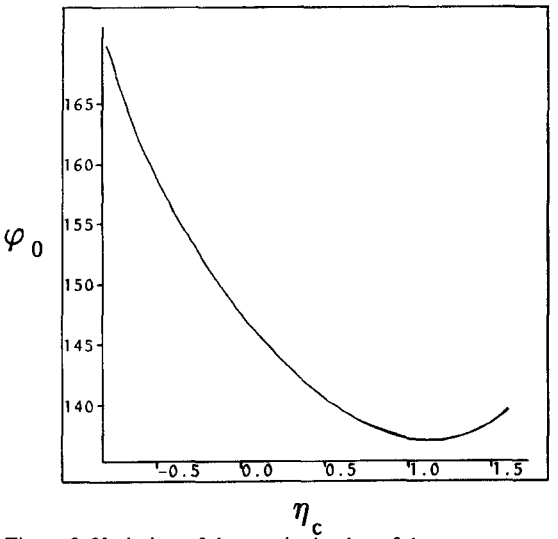

Figure 3. Variation of the required value of the true contact angle, φ_0, with the central profile curvature, η_c: depending on the value of φ_0, either no or two solutions exist (Ca = −0.1, ξ_c = 15).

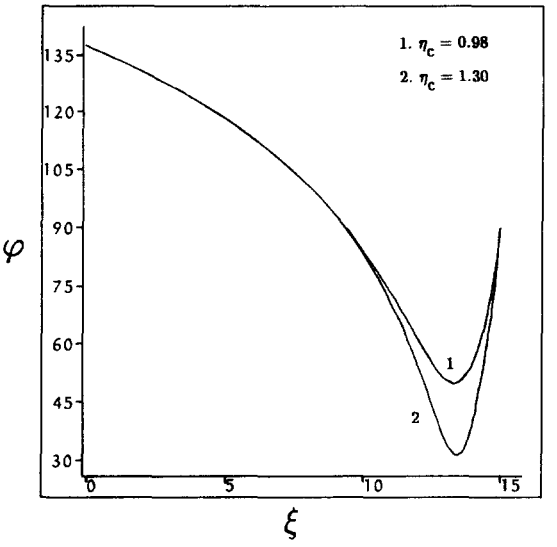

Figure 4. Meniscus profile for the two solutions (Ca = −0.1, ξ_c = 15, φ_0 = 137.2°).

To investigate the effect of system configuration on the shape of the receding menisci, menisci are examined between plates and in a tube for the case $\varphi_0 = 138.15°$, $\xi_c = 15$† and Ca = −0.1 (roughly the largest value of |Ca| for which a solution exists, as will be clear later). In the tube case the corresponding values of η_c and φ_d are 0.77 and 53°, while the corresponding values in the parallel-plate case are 1.00 and 41°. Although this difference appears considerable, the Ca required in the tube case to obtain $\eta_c = 1$ (with $\varphi_0 = 138.15°$ and $\xi_c = 15$) is in fact only marginally larger: −0.102. For smaller Ca this difference becomes even smaller, vanishing completely for Ca→0. Only the tube case will be examined further in detail in this article.

The meniscus equation [5] is solved for different η_c values. In figure 3, φ_0 is given as a function of η_c (where $\xi_c = 15$ and Ca = −0.1). In contrast with the situation for positive Ca, φ_0 is *not* a monotonic function of η_c but exhibits a minimum ($\varphi_{0,min} = 137.0°$). Evidently for $\varphi_0 < \varphi_{0,min}$ no solution of [5] exists, while for $\varphi_0 > \varphi_{0,min}$ there are two solutions. These two solutions for $\varphi_0 = 137.2°$ are shown in figure 4 ($\eta_c = 0.98$ for the upper curve and $\eta_c = 1.30$ for the other one). For the solutions having $d\varphi_0/d\eta_c > 0$ (see figure 3) it is found that $d\eta_c/dCa > 0$ (for constant φ_0 and ξ_c) and consequently that $d\varphi_d/dCa < 0$, which is contrary to experimental findings (Dussan 1979). The solutions for which $d\varphi_0/d\eta_c > 0$ will therefore be ignored. These solutions are presumably unstable and in that case not encountered in reality.

In general $\varphi_{0,min}$ is a function of the Ca and of ξ_c. In figure 5, $\varphi_{0,min}$ is given as a function of log(−Ca) for different ξ_c values. In a given system there thus exists a Ca (the Ca_{crit}) beyond which (in absolute value) there is no solution to the differential equation describing a stationary receding meniscus. Beyond the Ca_{crit} unsteady effects are therefore to be expected, probably resulting in a film of liquid being left behind.

4. DYNAMIC CONTACT ANGLES

In figure 6, φ_d is presented as a function of log(−Ca) for three values of ξ_c and of φ_0. The authors know of no data on φ_0 as a function of the contact line speed. Should φ_0 remain constant (equal to φ_s) then the curves in figure 6 would represent the actual variation of φ_d in a given system. Conversely the actual variation of φ_d provides information on any U-dependence of φ_0. More will be said on this subject in section 6.

†The order of magnitude corresponding to tubes of order 1 mm, assuming λ to be of the order of 1 nm.

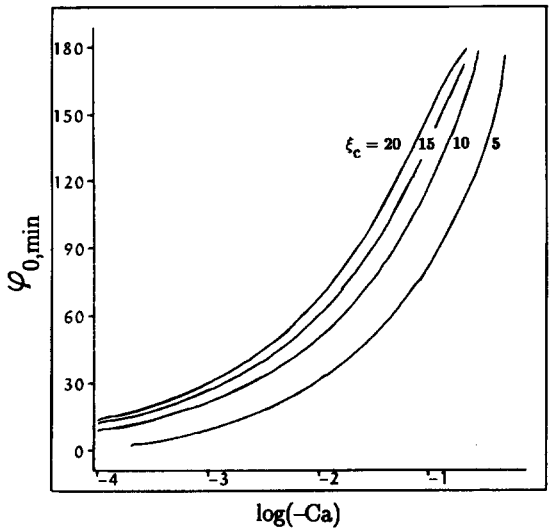

Figure 5. Variation of $\varphi_{0,min}$ with Ca for various system scales. Equivalently, the figure indicates the dependence of the Ca_{crit} on the true contact angle, φ_0.

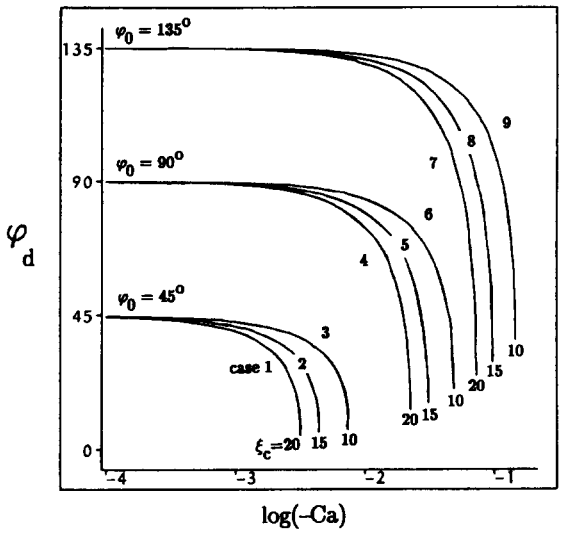

Figure 6. The dynamic contact angle presented as a function of the Ca for various true contact angles and system scales ($/\lambda$-values).

As noted earlier, various authors have defined the dynamic contact angle (especially in experimental work) as the angle which the circular profile of a moving meniscus seems to make with the wall. This definition is equivalent to [7] only if the greater part of the meniscus profile is circular. To obtain an impression of the extent of the central, circular portion of the meniscus, the meniscus is here defined as circular if it deviates from the extrapolation of the circular profile at the tube axis by $<3°$ (a not far-fetched uncertainty for measurements). The spherical fraction of the meniscus is given as a function of Ca in figure 7, defining this fraction as $(a - x_s)/a$, where x_s denotes the 3°-deviation point. Near the Ca_{crit} the predicted deviations of the meniscus from the spherical shape should be detectable in experiments, especially for larger true contact angles.

5. THE LOCAL-WEDGE APPROXIMATION

In figure 8 the dimensionless wedge-angle variation rate, $(d\varphi/\varphi)/(ds/w)$ is examined for Ca values close to the critical. In the wall region where the deviation from the spherical becomes major,

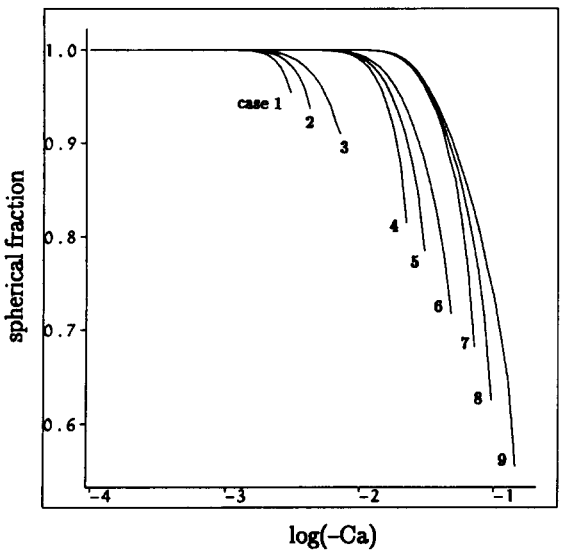

Figure 7. Spherical fraction of the meniscus for the cases studied in figure 6.

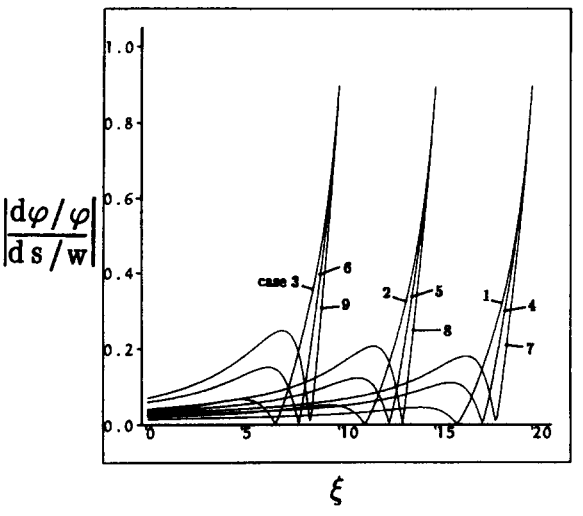

Figure 8. The dimensionless wedge-angle variation rate $|(d\varphi/\varphi)/(ds/w)|$ as a function of ξ for the cases studied in figure 6 ($\eta_c = 1$, Ca close to the critical value).

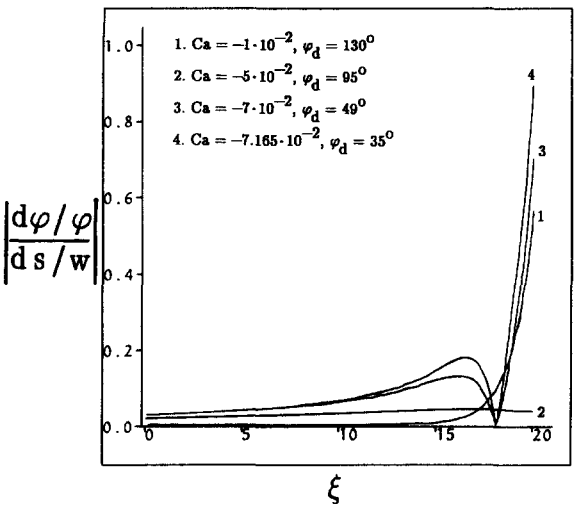

Figure 9. The dimensionless wedge-angle variation rate $|(d\varphi/\varphi)/(ds/w)|$ as a function of ξ for various Ca ($\xi_c = 20$, $\varphi_0 = 135°$).

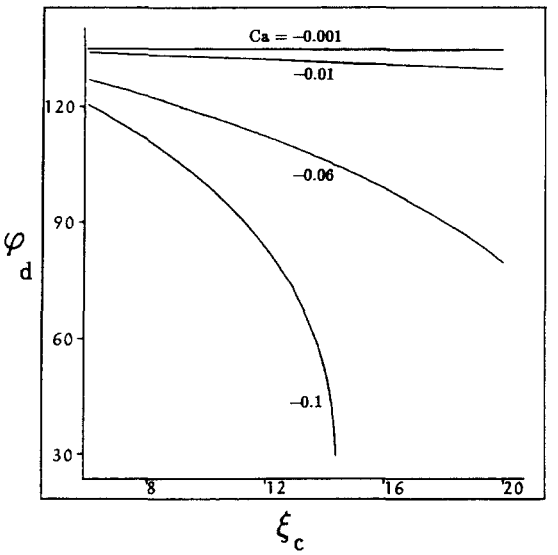

Figure 10. The dependence of the dynamic contact angle on the system scale ($/\lambda$-value) for various Ca ($\varphi_0 = 135°$).

this parameter is maximally about 0.2—a situation similar to that found in the advancing case for a Ca of order 10^{-1}, where close agreement with both numerical and experimental results is found. As discussed in paper I, requirement [4] is never satisfied in the central circular region, implying that the deviation from a circular profile predicted by [5] will not be accurate. Since this deviation is small, however, the total error remains acceptable. For smaller Ca, [4] is still better satisfied: figure 9.

There is thus good reason to expect that the solutions also provide a good approximation, the main uncertainty lying in the value of φ_0, as discussed below.

6. DYNAMIC CONTACT ANGLE DEPENDENCE ON SYSTEM SCALE AND TRUE CONTACT ANGLE

In figure 10 the predicted dynamic contact angle dependence on the system scale $a[/\lambda$ value, since $\xi_c = \ln(a/\lambda)]$ is presented for $\varphi_0 = 135°$ and various values of Ca. In contrast with the advancing case the dynamic contact angle is seen to depend strongly on ξ_c especially as the Ca_{crit} is approached.

In figure 11 the dynamic contact angle dependence on φ_0 is shown for $\xi_c = 15$ and various Ca. Again, in contrast with the advancing case, the dynamic contact angle is very sensitive to changes in φ_0, this sensitivity once more increasing as the Ca_{crit} is approached.

In view of the strong φ_0 dependence of φ_d, measurements of φ_d should provide an indication of the variation of the true contact angle with the line speed. In the next section a comparison of the predicted Ca_{crit} with recently obtained experimental values is undertaken.

7. COMPARISON WITH EXPERIMENTAL RESULTS

Receding contact lines in a tube geometry have been experimentally investigated recently by Quéré (1991). Drops of various alkanes were displaced inside a teflon capillary tube by applying a pressure difference over the drop and the Ca investigated at which the drop first leaves a film behind. Static contact angles for this system, deduced from microbalance measurements, exhibited considerable hysteresis, receding angles, φ_r, being around 20° less than advancing. Figure 12 compares the Ca_{crit} found by Quéré for different values of φ_r with predictions of the present model, assuming that

$$\varphi_0 = \varphi_r, \qquad [10]$$

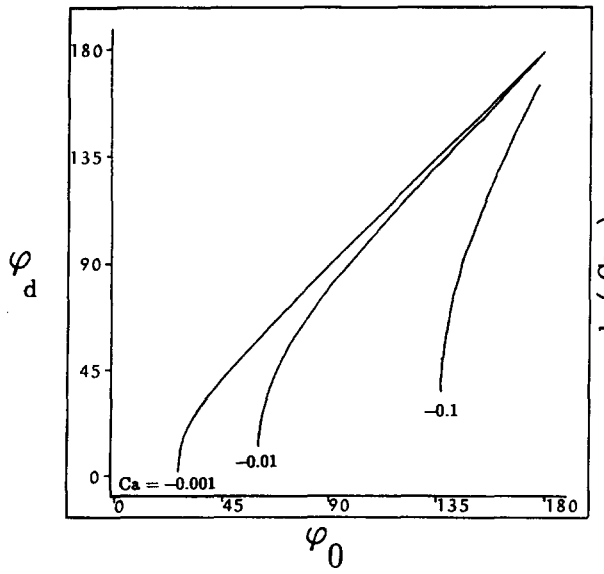

Figure 11. The dependence of the dynamic contact angle on the true contact angle at the wall for various Ca ($\xi_c = 15$).

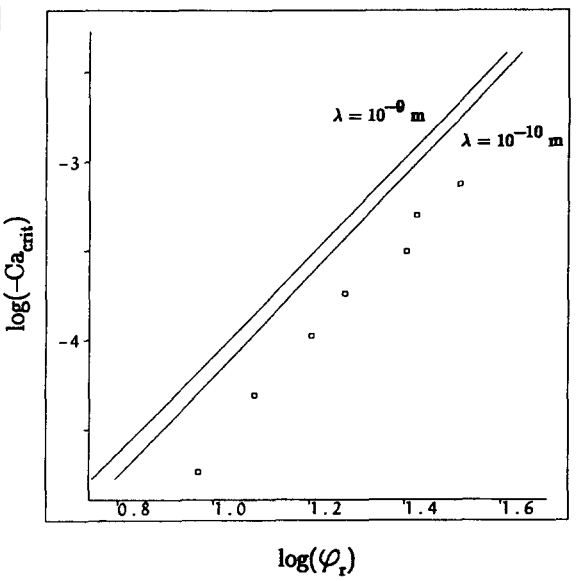

Figure 12. Comparison of the Ca_{crit} obtained experimentally by Quéré (1991) (□) with those predicted by the model (—) as a function of the (receding) static angle, assuming that $\varphi_0 = \varphi_r$ (φ_r in degrees).

for two values of λ: 10^{-9} and 10^{-10} m (the latter representing the lowest plausible value). While the order of magnitude and φ_r dependence of Ca_{crit} are well-predicted by the model, the values of Ca_{crit} appear† to be overpredicted by a factor of 2 or more.

Various possible explanations of this discrepancy present themselves. It may be related to the non-ideal nature of the solid surface concerned (as indicated by the substantial hysteresis observed in the static angles). It may reflect inaccuracies in the local-wedge approximation, though the success of this approximation in the advancing case suggests this is unlikely. Alternatively it may be indicative of a deviation of the true contact angle from the static (receding) value at the Ca concerned, good agreement with the measurements being obtained for a λ value of 10^{-9} m if it is supposed that

$$\varphi_0 = 0.68\varphi_r. \qquad [11]$$

The factor 0.68 would presumably increase as Ca decreases, becoming 1 in the static limit.

8. FINAL DISCUSSION

The present model, like others, predicts a maximum capillary number, Ca_{crit}, above which no stationary receding meniscus exists. Unlike other models, however, excepting that of de Gennes (1986), the limiting value of the dynamic contact angle at Ca_{crit} is not predicted to be zero, except in the limit of small true contact angle, φ_0. The portion of the meniscus which is significantly deformed from the spherical is, furthermore, predicted to be considerable unless φ_0 is small. The Ca_{crit} is predicted to exhibit a strong dependence on the system scale ($/\lambda$-value) and the true contact angle. It is this strong dependence which enables conclusions to be drawn from experiments regarding the values of φ_0 or λ. The comparison of the predictions of the model with the experiments of Quéré (1991) suggests that at the Ca_{crit} the true contact angle is significantly smaller than the static angle by a factor which is seemingly independent of the static contact angle for the alkane–teflon system concerned. Measurements of the Ca dependence of φ_d, would permit this factor to be evaluated for smaller Ca values.

†The error bounds indicated by Quéré (1991) on the lower φ_r values are greater than the discrepancy concerned; for the larger φ_r values, however, this is not the case.

REFERENCES

BLAKE, T. D. & RUSCHAK, K. J. 1979 A maximum speed of wetting. *Nature* **282,** 489–491.

BOENDER, W., CHESTERS, A. K. & VAN DER ZANDEN, A. J. J. 1991 An approximate analytical solution of the hydrodynamic problem associated with an advancing liquid–gas contact line. *Int. J. Multiphase Flow* **17,** 661–676.

BROCHARD, F., REDON, C. & RONDELEZ, F. 1988 Dewetting: the gravity controlled regime. *C. r. Acad. Sci. II* **306,** 1143–1146.

BROCHARD-WYART, F. & DAILLANT, J. 1990 Drying of solids wetted by thin liquid films. *Can. J. Phys.* **68,** 1084–1088.

BROCHARD-WYART, F., MEGLIO, J. M. & QUÉRÉ, D. 1987 Dewetting. Growth of dry regions from a film covering a flat solid or a fiber. *C. r. Acad. Sci. II* **304,** 553–558.

COX, R. G. 1986 The dynamics of the spreading of liquids on a solid surface. Part 1. Viscous flow. *J. Fluid Mech.* **168,** 169–194.

DUSSAN, V. E. B. 1979 On the spreading of liquids on solid surfaces: static and dynamic contact lines. *A. Rev. Fluid Mech.* **11,** 371–400.

DE GENNES, P. G. 1985 Wetting: statics and dynamics. *Rev. Mod. Phys.* **57,** 827–863.

DE GENNES, P. G. 1986 Deposition of Langmuir–Blodgett layers. *Colloid Polym. Sci.* **264,** 463–465.

HOPF, W. & GEIDEL, TH. 1987 The dynamic contact angle I. Dependence of the receding contact angle on velocity in the surfactant-containing three-phase system. *Colloid Polym. Sci.* **265,** 1075–1084.

PETROV, J. G. & RADOEV, B. P. 1981 Steady motion of the three phase contact line in model Langmuir–Blodgett systems. *Colloid Polym. Sci.* **259,** 753–760.

PETROV, J. G. & SEDEV, R. V. 1985 On the existence of a maximum speed of wetting. *Colloids Surf.* **13,** 313–322.

QUÉRÉ, D. 1991 On the minimal velocity of forced spreading in partial wetting. *C. r. Acad. Sci. II* **313,** 313–318.

REDON, C., BROCHARD-WYART, F. & RONDELEZ, F. 1991 Dynamics of dewetting. *Phys. Rev. Lett.* **66,** 715–718.

RILLAERTS, E. & JOOS, P. 1980 The dynamic contact angle. *Chem. Engng Sci.* **35,** 883–887.

SEDEV, R. V. & PETROV, J. G. 1988/89 Influence of geometry of the three-phase system on the maximum speed of wetting. *Colloids Surf.* **34,** 197–201.

SEDEV, R. V. & PETROV, J. G. 1991 The critical condition for transition from steady wetting to film entrainment. *Colloids Surf.* **53,** 147–156.

TELETZKE, G. F., DAVIS, H. T. & SCRIVEN, L. E. 1988 Wetting hydrodynamics. *Rev. Phys. Appl.* **23,** 989–1007.

VOINOV, O. V. 1976 Hydrodynamics of wetting. *Fluid Dynam.* **11,** 714–721.

VOINOV, O. V. 1978 Asymptote to the free surface of a viscous liquid creeping on a surface and velocity dependence of the angle of contact. *Sov. Phys. Dokl.* **23,** 891–893.